ORIGINAL ARTICLE

lajss.org
Latin American Journal of Solids and Structures

www.lajss.org

Experimental study of the seismic behavior of an existing bridge abutment located on soft clay deposits

Yong Yang[a]*, Shunsuke Tanimoto[a], Takaharu Kiriyama[a]

[a] Center for Advanced Engineering Structural Assessment and Research, Public Works Research Institute, Tsukuba, Ibaraki, 305-8516, Japan. Email: y-yang55@pwri.go.jp, s-tanimo@pwri.go.jp, kiriyama-t673bs@pwri.go.jp

* Corresponding author

http://dx.doi.org/10.1590/1679-78256024

Abstract

In this study, a dynamic centrifuge experiment is designed to investigate the seismic behavior of an existing bridge subjected to the earthquake-induced lateral movement of soft clay soil. The pile-supported bridge abutment at the movable bearing side is modeled at the 1/75 scale. The material and thickness of the soft clay layer are set as the experimental parameters. Under the effect of the lateral movement of the soft clay layer during base shaking, a collision between the bridge abutment wall and the girder occurs, and the bridge abutment wall is restrained at the top; however, the footing largely moves forward, resulting in the large backward inclination of the bridge abutment wall. In addition, it is confirmed that during base shaking, the pile bending moment largely increases due to the ground lateral movement and then remains nearly constant, even at the end of the base shaking phase. Furthermore, it is found that when the soft clay has a high shear strength, the ground lateral movement may cause a high pile earth pressure, resulting in the large corresponding internal bending moment on the pile sections; however, when the soft clay layer is very thick, the high pile earth pressure generally occurs locally, instead of along the whole pile length.

Keywords

existing bridge abutment, soft clay layer, lateral movement, seismic behavior, dynamic centrifuge experiment

Graphical Abstract

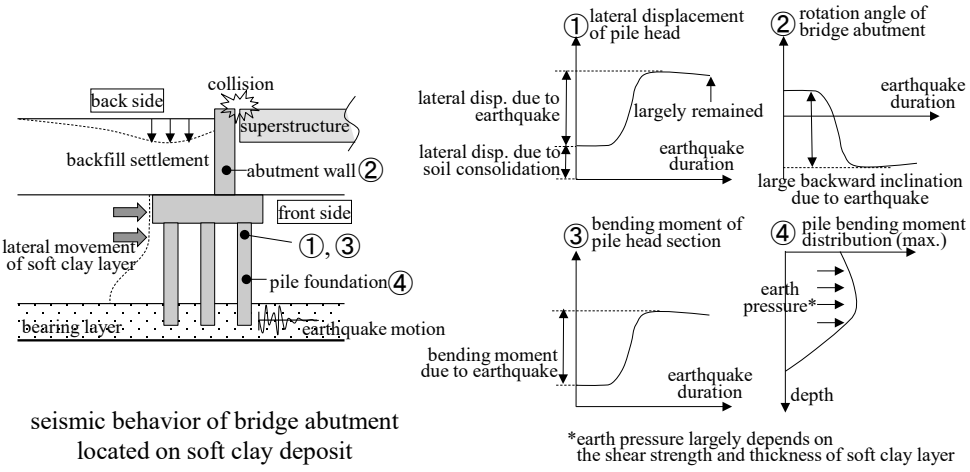

seismic behavior of bridge abutment located on soft clay deposit

Received: March 13, 2020. In Revised Form: April 03, 2020. Accepted: April 05, 2020. Available online: April 07, 2020.
https://doi.org/10.1590/1679-78256024

1. INTRODUCTION

Bridge damage reconnaissance and investigations conducted after earthquakes indicate that in addition to the superstructure inertial action, the surrounding ground failure can also cause damage to bridge structures. The most well-known ground failure is liquefaction. Saturated sand ground is most prone to fail due to liquefaction during an earthquake. In severe cases, ground liquefaction can also cause lateral flow acting on bridge foundations, resulting in destructive damage to bridge structures. Potential bridge damage induced by ground liquefaction has been recognized as an important issue for bridge design. However, in addition to saturated sand ground, soft clay ground can also be expected to fail during earthquakes and can cause potential damage to bridge structures. In particular, strong earthquake motions can trigger the lateral movement of soft clay deposits and result in destructive damage to bridge structures, similar to ground liquefaction. For existing bridges designed with outdated standards, the considered seismic load is generally small, and the gap between the abutment wall and superstructure is always narrow. As shown in Figure 1, under the lateral movement of the soft clay layer during an earthquake, the bridge abutment is expected to move forward. A collision between the abutment wall and superstructure is possible, but this effect has not been considered in bridge design. The corresponding external and internal force distributions of both the bridge abutment and the superstructure may be quite different from those assumed in the design stage. Consequently, in some severe cases, unexpected bridge damage may occur and impede relief activities after an earthquake. Figure 2 shows an example of a damaged pile foundation of one existing bridge abutment in 2011 off the Pacific coast of the Tohoku Earthquake of Japan (Public Works Research Institute 2014, 2018) due to the lateral movement of the thick soft clay layer. Thus, to accurately evaluate the seismic performance of the existing bridges constructed on the soft clay deposits, especially with a small gap between the abutment wall and superstructure, it is necessary to consider the effect of the ground lateral movement.

Liquefaction phenomena have received considerable attention in previous studies, and numerous research studies have been carried out to investigate the liquefaction effect on the seismic performance of structures (e.g., Wilson et al. 2000; Brandenberg et al. 2005; Shirato et al. 2006; Chang 2007; El-Sekelly et al. 2016; Su et al. 2016; Zhang et al. 2020). However, relatively little attention has been paid to the seismic performance of structures constructed on soft clay deposits. For example, in the aspect of laboratory tests, to analyze seismic soil-pile-structure interactions in soft clay, Boulanger et al. (1999) conducted dynamic centrifuge model tests to evaluate a dynamic beam on a nonlinear Winkler foundation analysis method.

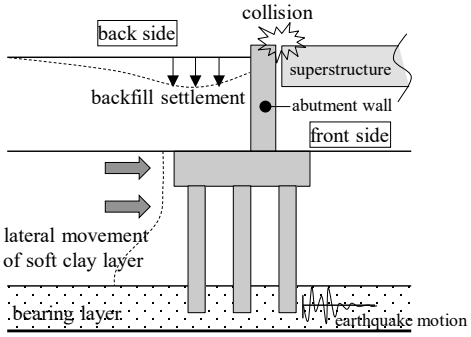

Figure 1 Effect of the lateral movement of soft clay deposits on the seismic behavior of a bridge

Figure 2 Bridge pile foundation damaged at the upper end due to the lateral movement of the soft clay deposit

In the dynamic centrifuge model tests, a single-pile-supported system consisting of a superstructure mass attached to an extension of the pile was designed. Chandrasekaran et al. (2010) conducted two-way cyclic lateral load tests on model pile groups embedded in soft marine clay to investigate the pile group behavior. The pile groups have different length-to-diameter ratios and spacing-to-diameter ratios. Banerjee et al. (2014) carried out centrifuge tests to examine seismic effects on fixed-head, end-bearing piles installed through soft clay. Other previous studies related to the seismic response of pile foundations in soft ground can be found in the literature (Wilson et al. 1997; Wilson 1998; Boominathan and Ayothiraman 2006; Zhang et al. 2017; Garala and Madabhushi 2019; Yang et al. 2019). In addition to these laboratory tests, the measured seismic response data of a real bridge constructed on soft clay ground were used to develop finite element models to assess the soil-foundation-support performance under long-term conditions (Mayoral et al. 2009). The effects of soil improvement on the seismic resistance of pile foundations in soft clay have also been investigated in a few studies (e.g., Meymand 1998; Brown et al. 2001; Mayoral et al. 2005; Rollins and Brown 2011; Fleming et al. 2016).

In most of the laboratory tests mentioned above, only a single pile or a pile group is modeled, and the superstructure is ignored or simply modeled as a mass block. However, as indicated in the previous study (Qiu et al. 2020), not only the bridge foundation but also the bridge superstructure can exert a significant restraining effect on lateral ground deformations. That is, the bridge response is highly dependent on the bridge-ground system, not only the bridge foundation. Thus, based on previous studies, it is difficult to understand the global seismic behavior of bridge structures constructed on soft clay deposits, especially for the issue shown in Figure 1.

This research aims to develop an evaluation method for the seismic performance of existing bridges located on soft clay deposits, which are potentially subjected to earthquake-induced lateral movements (Figure 1). As the first step, to provide basic knowledge for this research, a dynamic centrifuge experiment is designed to investigate the seismic behavior of bridge abutments subjected to earthquake-induced lateral movement of a soft clay layer. Compared with previous studies, not only the bridge abutment but also the bridge superstructure is modeled in the centrifuge experiment.

In this paper, the seismic behavior of pile-supported bridge abutments located on soft clay layers with different materials and thicknesses is reported. First, the experimental program, including the experimental parameters, the bridge abutment model design, the experimental procedure, and the experimental measurement, is introduced. Second, the seismic behavior of the front-side and back-side ground is explained. The effects due to the differences in the soft clay layer on the seismic behavior of the ground are also discussed. Third, the seismic behavior of the bridge abutment is illustrated. The external earth pressure of the piles is also discussed based on the internal bending moment distribution.

2. EXPERIMENTAL PROGRAM

Since the similarity law of the stress-strain relation of the soil between the model and prototype can be easily satisfied, centrifuge loading testing is applied to geotechnical structure models. The centrifuge loading test simulates the actual stress-strain conditions in the field by increasing the g field. In addition, the cost of a centrifuge experiment is also less than that of a 1 g shaking table loading test. Thus, in this research, the seismic behavior of a bridge abutment subjected to earthquake-induced lateral movement of the soft clay layer is investigated by a dynamic centrifuge experiment rather than a 1 g shaking table experiment. Further information regarding centrifuge loading tests can be found in the following literatures (Schofield 1980; Madabhushi 2014).

2.1 Experimental parameters

In the dynamic centrifuge experiment, the pile-supported bridge abutment at the movable bearing side is modeled. The experimental scale is set to 1/75 considering the centrifuge loading device capacity. As shown in Table 1, to investigate the effect of the lateral movement of the soft clay layer on the seismic behavior of the bridge abutment, three cases are designed with different materials and thicknesses of the soft clay layer. In Case 1, designated as the basic case, the soft clay layer is 160 mm thick at the model scale and is made of kaolin clay material. Case 2 has a soft clay layer made of sumi clay material, with the same thickness as that in Case 1. Case 3 has a soft clay layer that is made of kaolin clay material and that is 240 mm thick, which is thicker than that of Case 1. The material properties of the kaolin and sumi clay are shown in Table 2. The consolidation test results show that the sumi clay material has a greater consolidation yield stress than that of the kaolin clay. Furthermore, the consolidated-drained triaxial compression test shows that the sumi clay also has greater shear strength.

Table 1 Experimental parameters (model scale).

Case	ground conditions						pile conditions	
	backfill layer		soft clay layer		bearing layer		pile group	diameter
	thickness	material	thickness	material	thickness	material		
1	160 mm	silica sand	160 mm	kaolin clay	80 mm	silica sand	3 × 4	14 mm
2				sumi clay*				
3			240 mm	kaolin clay				

*A mineral powder made by Sumitomo Osaka Cement Co., Ltd., Japan.

Table 2 Material properties of the kaolin and sumi clay.

material		kaolin clay	sumi clay
consolidation test	compression index C_c	0.336	0.195
	consolidation yield stress (kN/m^2)	66.9	375.0
consolidated-drained triaxial compression test	cohesion c (kN/m^2)	13.3	46.1
	friction angle ϕ (°)	9.2	16.7

The three cases have the same backfill layer thickness and bearing layer thickness. Silica sand with a mean particle size equal to 0.29 mm is used to construct these two layers. The relative densities of the backfill layer and the bearing layer are 80% and 90%, respectively.

The three cases also have the same pile conditions. The pile foundation is designed with a 3 × 4 pile group layout, and the pile diameter is equal to 14 mm at the model scale.

The acceleration wave 2-I-I-3, which is chosen from the acceleration wave database prescribed in the Design Specifications for Highway Bridges of Japan (Japan Road Association 2017) for bridge dynamic numerical analysis, is adopted as the input earthquake motion, considering the similarity law between the model and prototype. Due to the limitation of the loading device capacity, the acceleration amplitude is reduced to 80% in the centrifuge experiment. The input acceleration wave is shown afterwards, along with other ground acceleration responses (see Section 3.1).

2.2 Bridge abutment model

Figure 3 shows the schematic diagram of the bridge abutment model for Case 1, along with the surrounding ground set in the rigid soil container. Cases 2 and 3 have schematic diagrams of the bridge abutment model that are similar to the schematic diagram of Case 1. The soil container has dimensions of 1500 mm × 300 mm × 500 mm (length × width × height). In addition to the bridge abutment model with the 3 × 4 pile group, bridge abutments with 3 × 2 pile group are also set at the two sides of the central model to reduce the adhesion effect between the soil container wall and the soft clay soil. A sponge material is also installed between the central and side bridge abutment models to reduce the friction effect. To simulate the collision between the bridge abutment at the movable bearing side and the superstructure, a simply fabricated girder is set by fixing one end to the soil container wall. The spacing between the girder end and the bridge abutment wall is set to 1 mm at the model scale.

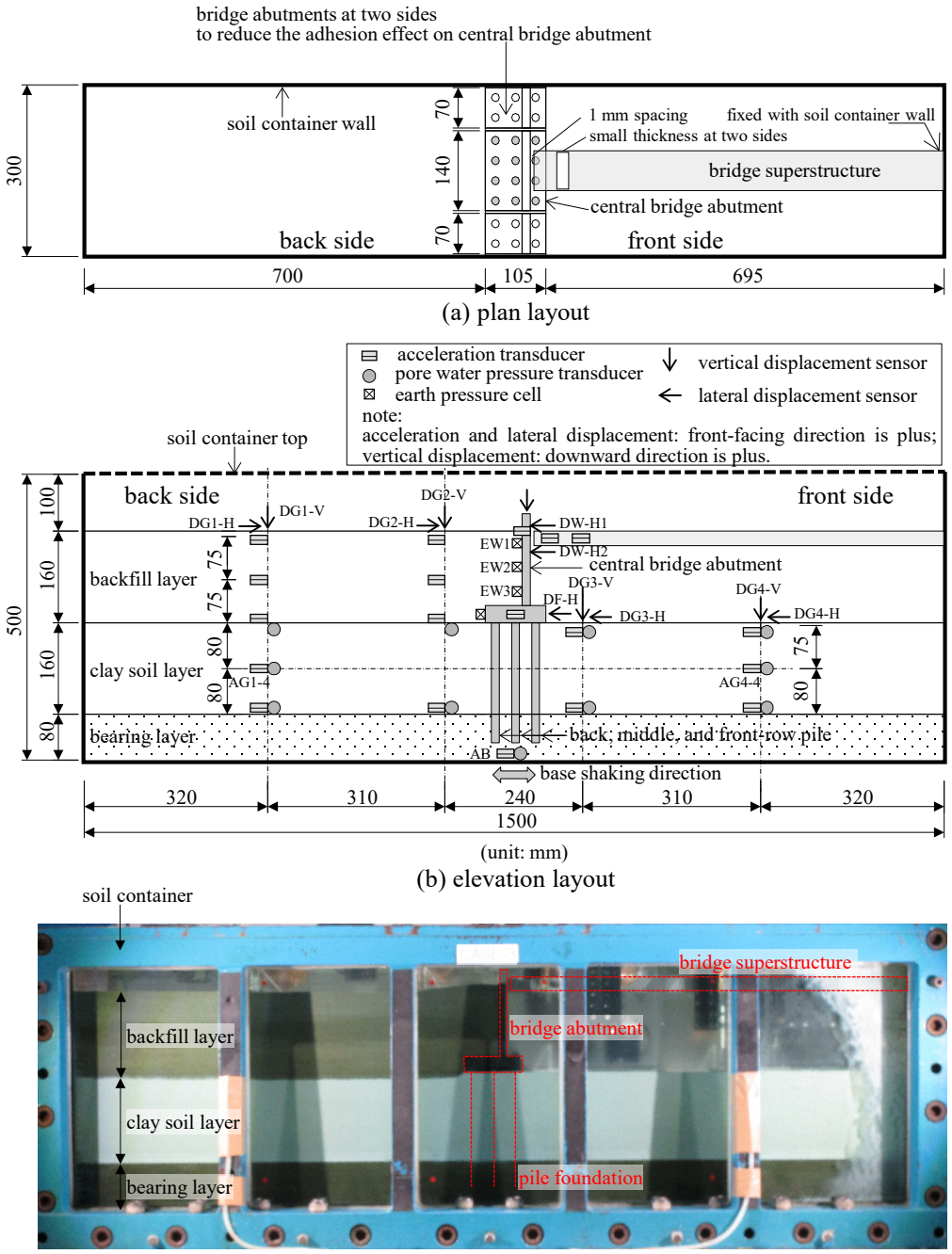

Figure 3 Bridge abutment model set in the soil container (Case 1)

Figure 4 shows the details of the central bridge abutment for the three cases. The abutment wall model has dimensions of 140 mm × 160 mm × 15 mm (length × height × thickness), and the footing model has dimensions of 140 mm × 105 mm × 30 mm (length × width × thickness) in three directions. Both the abutment wall and the footing models are made of aluminum material.

Aluminum pipes with a 14 mm outer diameter and a 1 mm wall thickness are used to make the pile models for the three cases (Figure 5). The material properties of the aluminum pipe are shown in Table 3. Three cases have different pile lengths. Cases 1 and 2 have the same pile length of 210 mm, which is measured from the footing bottom; Case 3 has a pile length of 290 mm. In all three cases, the pile head is rigidly fixed to the footing model; the lower end is inserted into the bearing layer with the embedment length equal to 50 mm. Additionally, the pipe spacing shown in Figure 4 is 35 mm in all three cases, which is equal to two and half times the pile diameter.

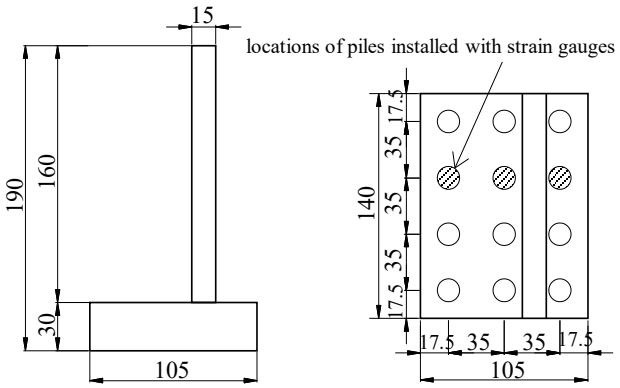

(a) front view (b) top view

Figure 4 Details of the central bridge abutment model

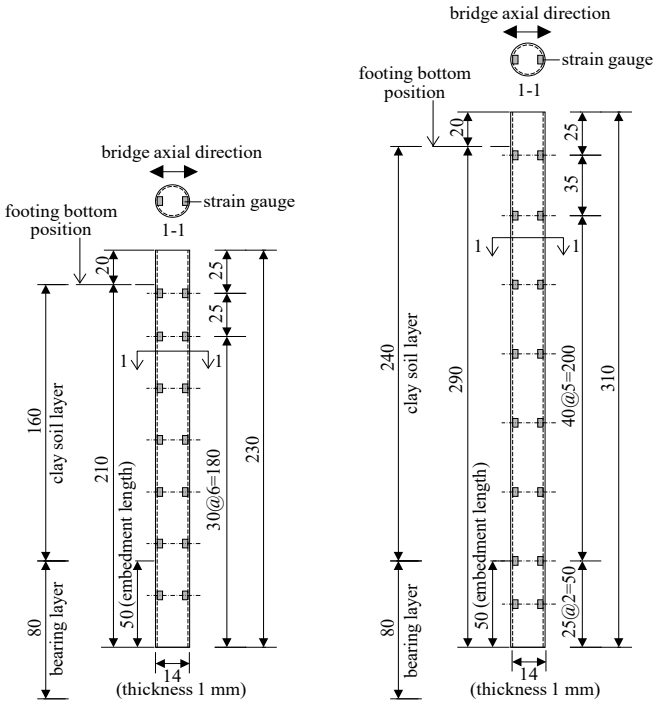

(a) Cases 1 and 2 (b) Case 3

Figure 5 Details of the pile models

Table 3 Material properties of the aluminum pipe.

tensile test	yielding strength* (N/mm²)	yielding strain (μ)	Young's modulus (N/mm²)
1	195.8	4879	69.7
2	195.2	4853	68.4
3	199.0	4853	69.5
average	196.7	4862	68.9

*The yielding strength is obtained by the 0.2% offset strain method.

2.3 Experimental procedure

In this centrifuge experiment, the installation sequence of the ground model and the bridge abutment model is shown in Figure 6. (1) The bearing layer is installed at the bottom of the soil container. Then, the soft clay slurry is added into the soil container after the placement of the pile models. (2) The soft clay slurry is consolidated with the overburden load in a 75 g field. (3) After 90% consolidation of the soft clay layer is finished, the consolidated soft clay layer is cut down to the designed thickness in a 1 g field. Then, the footing and the abutment wall model are installed,

and the backfill layer as well as the bridge superstructure is added. (4) The completed ground model installed with the bridge abutment model is consolidated again in a 75 g field until 90% consolidation is reached. (5) After 90% consolidation of the soft clay layer, the spacing between the superstructure and the abutment wall model is adjusted to approximately 1 mm in a 1 g field. (6) In a 75 g field, dynamic loading in the longitudinal direction of the soil container is conducted under the undrained condition.

2.4 Experimental measurement

As shown in Figure 3(b), several types of transducers are placed on the bridge abutment model as well as in the surrounding ground. These transducers include acceleration transducers, pore water pressure transducers, earth pressure cells, and displacement sensors. After the centrifuge experiment, the ground is also cut to investigate the residual displacement at different depths by measuring the movement of the measurement mark buried in the ground.

In addition, strain measurements are also conducted for the bridge superstructure, the abutment wall, and the piles. The bridge superstructure model is made with a small thickness near the left end to accurately measure the axial strain and to evaluate the axial force due to the collision with the abutment wall. The bending strain at the base of the abutment wall is also measured to evaluate the base bending moment. To evaluate the bending moments acting on the pile sections, three piles shown in Figure 4 are chosen to install strain gauges for each case, and the strain gauge arrangement is shown in Figure 5. The strain gauges are placed on the inner surface of the pile models. Cases 1 and 2 have seven sections and Case 3 has eight sections installed with strain gauges.

With regard to the experimental data collection during the dynamic loading phase, for the earth pressure, displacement, and strain, the response observed during the second stage of clay soil consolidation is considered to set the initial values; for the acceleration and pore water pressure, the initial values are set equal to zero. The measurement duration during the dynamic loading phase is 4 s, and the data acquisition frequency is 10 kHz.

Note that in the following sections, to intuitively understand the seismic behavior of the bridge abutment subjected to the lateral movement of the soft clay layer, the experimental results are given and illustrated at the prototype scale. The main scaling relations between the prototype and model are shown in Table 4.

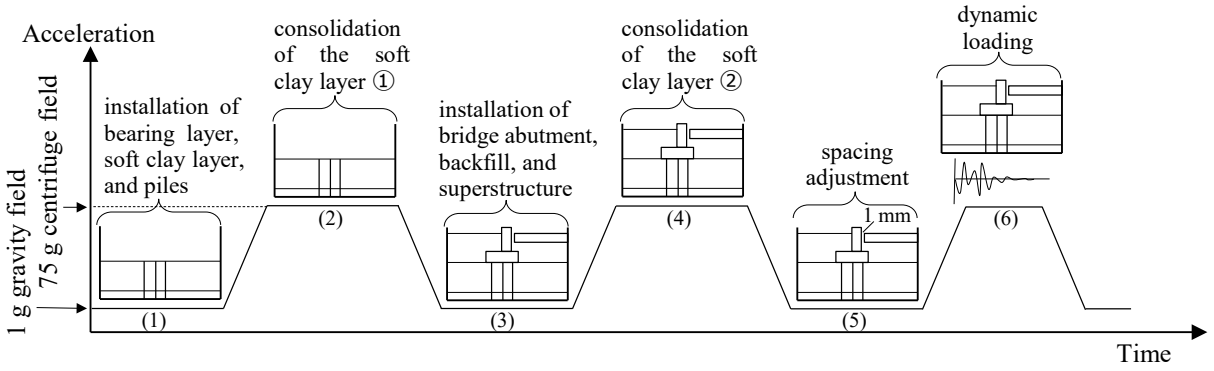

Figure 6 Experimental procedure

Table 4 Scaling relations between the prototype and model.

	length, displacement	time (dynamic)	acceleration		force	moment	stress, pressure	strain
			centrifuge	shaking				
prototype	1	1	1	1	1	1	1	1
model	1/N	1/N	N	N	$(1/N)^2$	$(1/N)^3$	1	1

3. EXPERIMENTAL RESULTS AND DISCUSSION OF THE GROUND BEHAVIOR

3.1 Acceleration response

The acceleration response of the soft clay layer is discussed here. The three cases have similar experimental results. The measured time histories of the acceleration response (AG1-4 and AG4-4) at the mid-depth of the soft clay layer of Case 1 and the input earthquake motion (AB) measured at the soil container bottom are shown in Figure 7 as an example.

In the soft clay layer at the back side of the abutment wall, the acceleration amplification phenomenon is observed over the whole shaking period. However, in the soft clay layer at the front side of the abutment wall, the acceleration amplification phenomenon is observed only before approximately 75 s; after 75 s, acceleration attenuation clearly occurs. This finding can be explained by the rigidity degradation of clay soil due to cyclic shearing during base shaking. In particular, for the soft clay layer at the front side of the abutment wall, due to the small restraint pressure, the cyclic shearing effect on the rigidity degradation is more influential.

3.2 Displacement response

The measured lateral displacement and settlement at the ground surface in Case 1 are shown in Figure 8(a) and (b), respectively. The experimental results at the beginning of the base shaking phase (0 s), for the lateral displacement and the settlement caused by the clay soil consolidation before base shaking, show no obvious difference among the lateral displacements at points DG1 to DG4; however, due to the different overburden loads of the soft clay layer on the two sides, the settlements (DG1-V and DG2-V) on the back side are clearly larger than those on the front side. During the base shaking from 50 to 150 s, the lateral displacement and the settlement clearly increase, except for the settlement (DG3-V and DG4-V) at the front side. In particular, the lateral displacement (DG3-H) near the abutment wall at the front side and the settlement (DG2-V) near the abutment wall at the back side increase greatly. At the end of the base shaking phase of approximately 300 s, both the residual lateral displacement and settlement nearly reach their maximum values obtained during base shaking. With regard to the change tendency and the magnitude relation of the lateral displacements and the settlements, Cases 2 and 3 have results similar to those of Case 1.

Figure 9(a) and (b) shows comparisons of the lateral displacement DG3-H and the settlement DG2-V among the three cases, respectively. Due to the high shear strength of the clay soil, the increase in DG3-H during the base shaking phase in Case 2 is clearly less than that observed in Case 1. However, the increase in DG3-H during the base shaking phase in Case 3 is less than that of Case 1, although Case 3 has a thicker soft clay layer. The reason for this will be further investigated based on the ground residual lateral displacement shown in Figure 10. For settlement DG2-V in the three cases, the results at 0 s indicate that the shear strength and thickness of the soft clay layer can considerably affect the settlement during the consolidation phase; however, the increases in DG2-V during the base shaking phase in the three cases are approximately equal to each other, and the effects of the shear strength and thickness of the soft clay layer are not clearly confirmed.

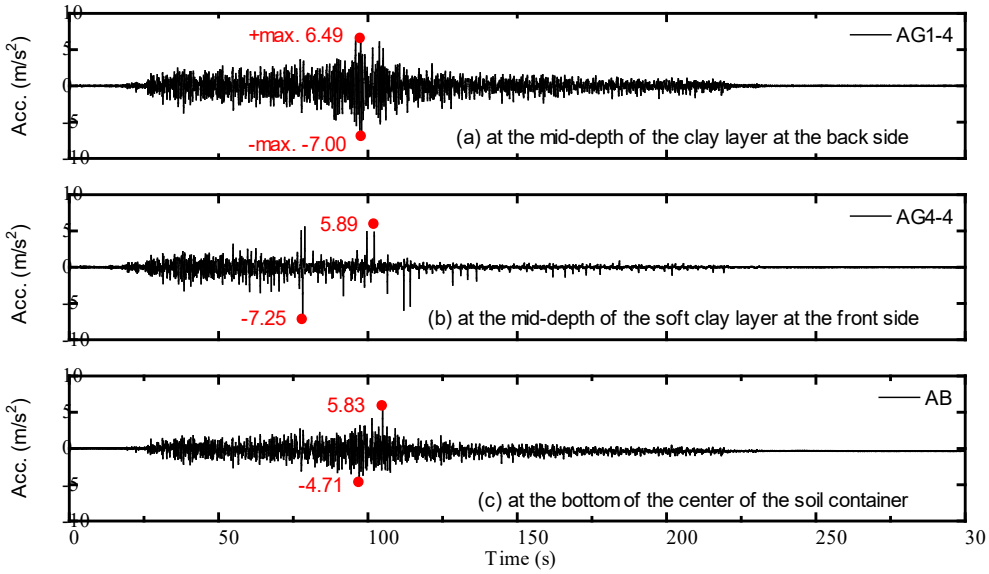

Figure 7 Time histories of the acceleration response

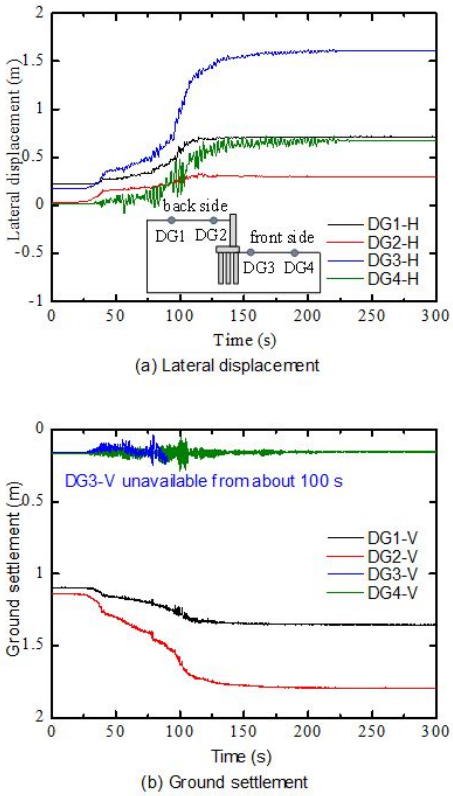

Figure 8 Time histories of the lateral displacement and the settlement at the ground surface

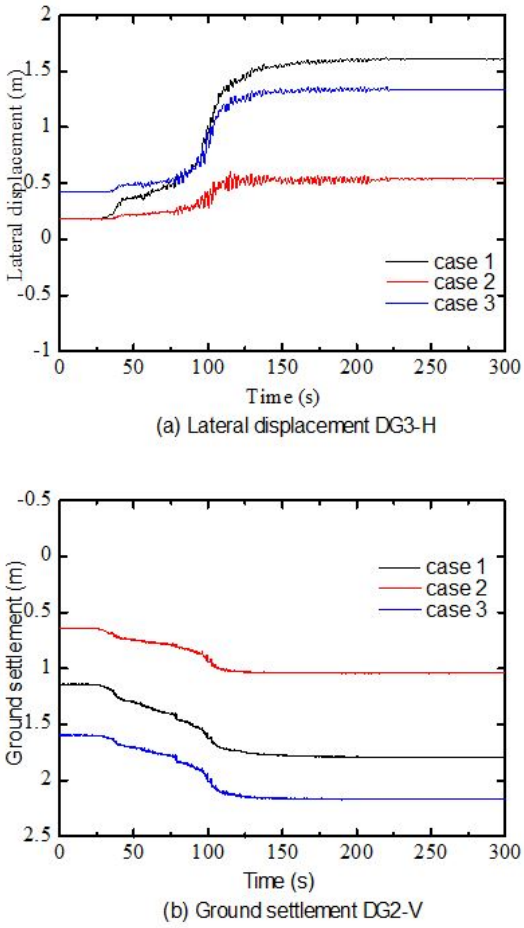

Figure 9 Comparisons of the results of the lateral displacement DG3-H and the settlement DG2-V for the three cases

3.3 Residual displacement

The ground residual displacement at different depths, which is investigated after base shaking by measuring the movement of the measurement mark buried in the ground, is shown in Figure 10 for the three cases. The three cases similarly show that due to the consolidation and base shaking, the settlement behind the abutment wall occurs over a large area in the backfill layer. The residual lateral displacement of the soft clay layer at the front side near the pile foundation is clearly larger than that at the other locations.

Due to the high shear strength of the clay soil, both the residual lateral displacement and the settlement in Case 2 are smaller than those in Case 1. Due to the larger thickness of the soft clay layer, the settlement behind the abutment wall in Case 3 is larger than that of Case 1. The residual lateral displacement of the soft clay layer in Case 3, especially at the front side of the abutment wall, is clearly larger than that in Case 1. At the front side near the abutment wall, the maximum residual lateral displacements of Cases 1 and 3 occur at the ground surface and under the ground surface, respectively. That is, the soft clay layers in Cases 1 and 3 have different deformation behaviors, which largely depend on the soft clay layer thickness. Thus, the result shown in Figure 9(a) that the lateral displacement DG3-H in Case 3 at the ground surface is less than that of Case 1 can be explained.

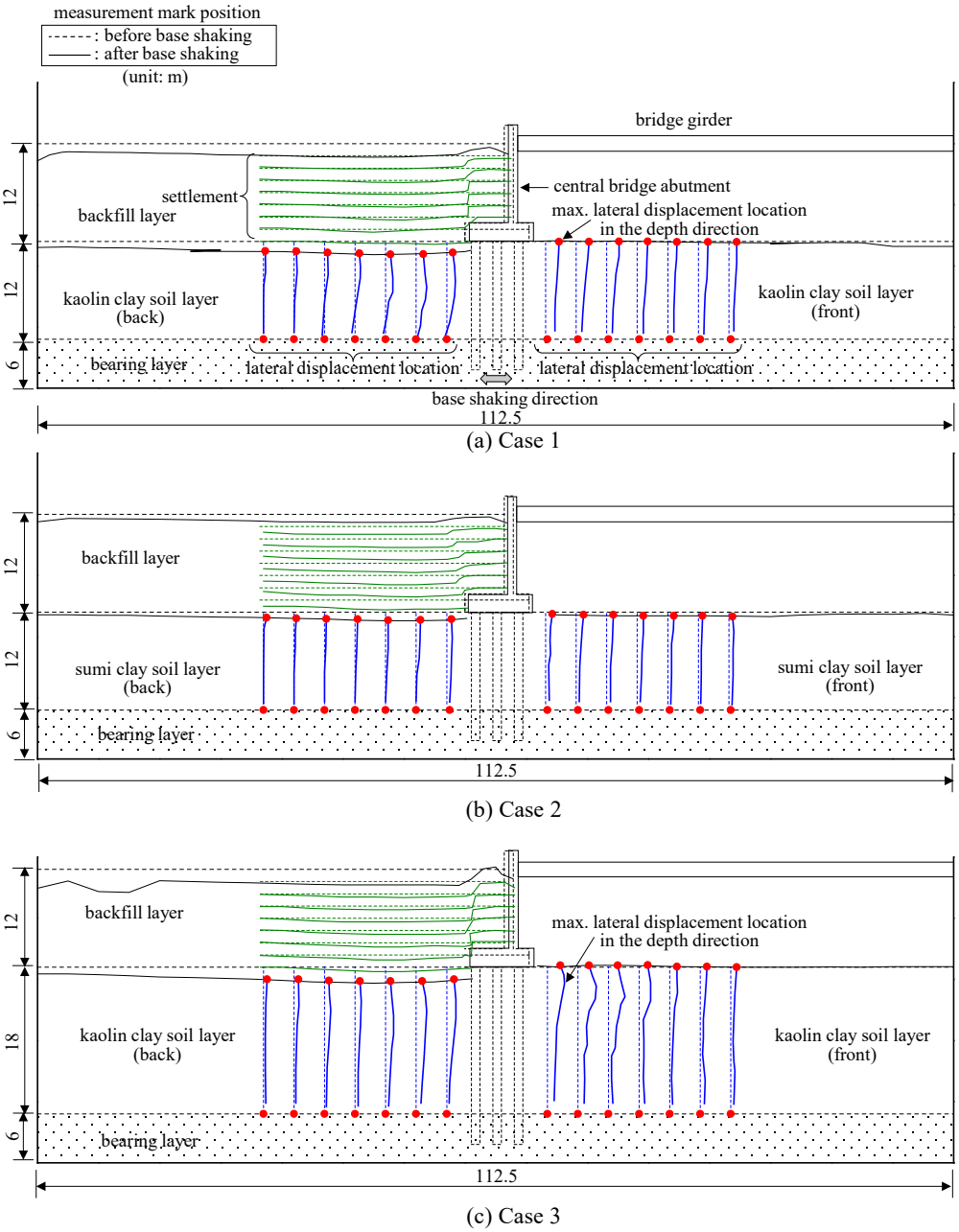

Figure 10 Ground residual displacement after the base shaking

4. EXPERIMENTAL RESULTS AND DISCUSSION OF THE BRIDGE ABUTMENT BEHAVIOR

4.1 Lateral displacement response

Figure 11 shows the time histories of the lateral displacements at different heights of the bridge abutment wall in Case 1. At the beginning of the base shaking phase (0 s), the lateral displacement at the top (DW-H1) is larger than that at the footing location (DF-H), showing that the bridge abutment wall inclines forward due to the consolidation effect. From the base shaking time of approximately 50 s, the lateral displacement at the footing location (DF-H) is larger than that at the abutment wall top (DW-H1), showing the inverse magnitude relation of the lateral displacements. That is, the bridge abutment wall inclines backward during base shaking because the abutment wall is restrained at the top due to collision with the bridge girder; however, since the pile foundation is subjected to lateral movement of the soft clay layer, the lateral displacement at the footing location sharply increases. Cases 1, 2 and 3 exhibit similar results in terms of the lateral displacement of the bridge abutment.

4.2 Rotation response

Based on the lateral displacements DW-H1 and DW-H2, the rotation angle of the bridge abutment is evaluated and shown in Figure 12 for the three cases. At the beginning of the base shaking phase (0 s), Case 2 exhibits a forward inclination that is equal to that observed in Case 1; however, due to the high shear strength of the clay soil, the change in the rotation angle during the base shaking phase in Case 2 is clearly smaller than that of Case 1. Although Case 3 exhibits a larger forward inclination than Case 1 at the beginning of the base shaking phase, their maximum backward inclination angles during base shaking are almost identical; a larger change in the rotation angle is demonstrated in Case 3 during the base shaking phase. In all three cases, the residual rotation angles are almost equal to their maximum value obtained during the base shaking phase.

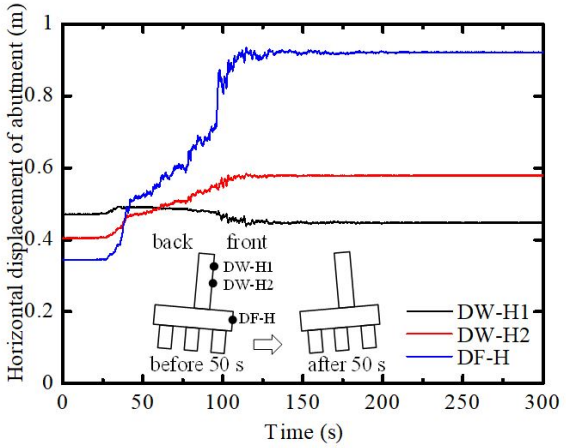

Figure 11 Lateral displacement of the bridge abutment

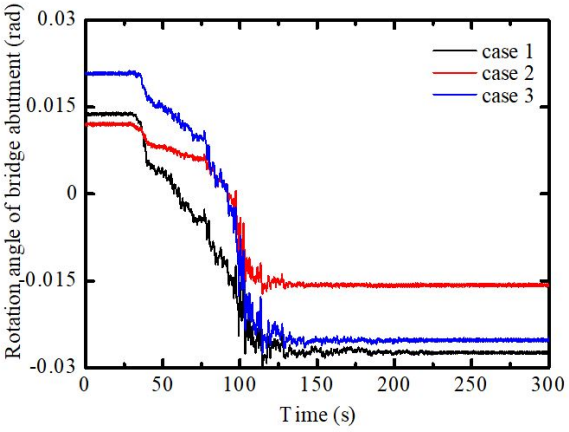

Figure 12 Rotation angle of the bridge abutment

4.3 Comparison between the time histories of the internal and external forces acting on the bridge abutment

Figure 13 shows the time histories of the internal and external forces acting on the bridge abutment and a close-up view of some of these results. The internal forces, which are evaluated based on the measured strain, include the girder axial force, the bending moment acting on the base of the abutment wall, and the pile bending moment. The external forces include the measured earth pressure acting on the abutment wall and the pile earth pressure. The pile earth pressure is evaluated based on the pile bending moment distribution by the second derivative method. Further information regarding the second derivative method can be found in the literature provided (Port and Airport Research Institute 2003).

As shown in Figure 13(a), over the whole base shaking phase, both the internal forces and the external forces gradually increase from 25 s and reach the maximum response at approximately 100 s, showing a similar increasing tendency. The time histories of the internal forces also show that under the lateral movement of the soft clay layer, the bridge girder is in the compression state, and the bridge pile foundation as well as the abutment wall is in the bending state.

As shown in Figure 13(b), the close-up view of the above time histories from 85 to 95 s indicates that the internal and external forces almost simultaneously reach their peak. The external earth pressures at EW1 and EW2 are clearly larger than those at EW3. At the upper location EW1, the calculated earth pressure coefficient nearly reaches 10 at approximately 91.5 s. This difference occurs because under the effect of the collision between the abutment wall and the girder, the relative displacements between the abutment wall and the backfill soil at EW1 and EW2 are larger than those at EW3.

4.4 Pile bending moment distribution

The pile bending moment distributions, which are evaluated based on the measured axial strain, are shown in Figure 14 for the three cases. By comparing the bending moments at the beginning of the base shaking phase (0 s) and at the maximum response point during the base shaking, the bending moment in the three cases largely increases when subjected to the base shaking-induced lateral movement of the soft clay layer. In addition, the results of the three cases similarly show that the bending moment generally persists, even at the end of the base shaking phase (299.9925 s).

At the maximum response point, the bending moment of the back-row pile in each case is larger than that of the middle- and front-row piles. Furthermore, the second derivative result (i.e., curve curvature) of the pile bending moment distribution curve can be considered corresponding to the external pile earth pressure. As shown in Figure 14, the curvature of the bending moment distribution curve of the back-row pile in each case is larger than that of the middle- and front-row piles. In other words, under the lateral movement of the soft clay layer, the back-row pile suffers a larger earth pressure than the middle- and front-row piles.

Although the ground displacement and the abutment rotation angle in Case 2 are clearly smaller than those in Case 1, Figure 14(a) and (b) shows that Case 2 does not have a clear tendency for the pile bending moment to be smaller than that in Case 1 at the maximum response point. This effect can be explained from the aspect of the pile earth pressure magnitude. The curvature of the pile bending moment distribution curve in Case 2, especially for the back-row pile, is clearly larger than that in Case 1, showing the greater pile earth pressure in Case 2. For a pile-supported bridge abutment constructed on the soft clay layer with high shear strength, the lateral movement of the soft clay layer may induce a high external earth pressure on the piles during an earthquake.

Although the soft clay layer in Case 3 is thicker than that of the basic Case 1, Figure 14(a) and (c) shows that the bending moments at the pile head section of the two cases are generally equal at the maximum response point. This result can be explained from the aspect of the acting scope of pile earth pressure. The bending moment distribution indicates that the greater earth pressure in Case 3 is limited to the back-row pile at a depth of approximately 6 m, instead of occurring along the whole pile length. In other words, for a pile-supported bridge abutment constructed on a thick soft clay layer, a high earth pressure may concentrate at a certain position along the piles during an earthquake, rather than along the whole pile length.

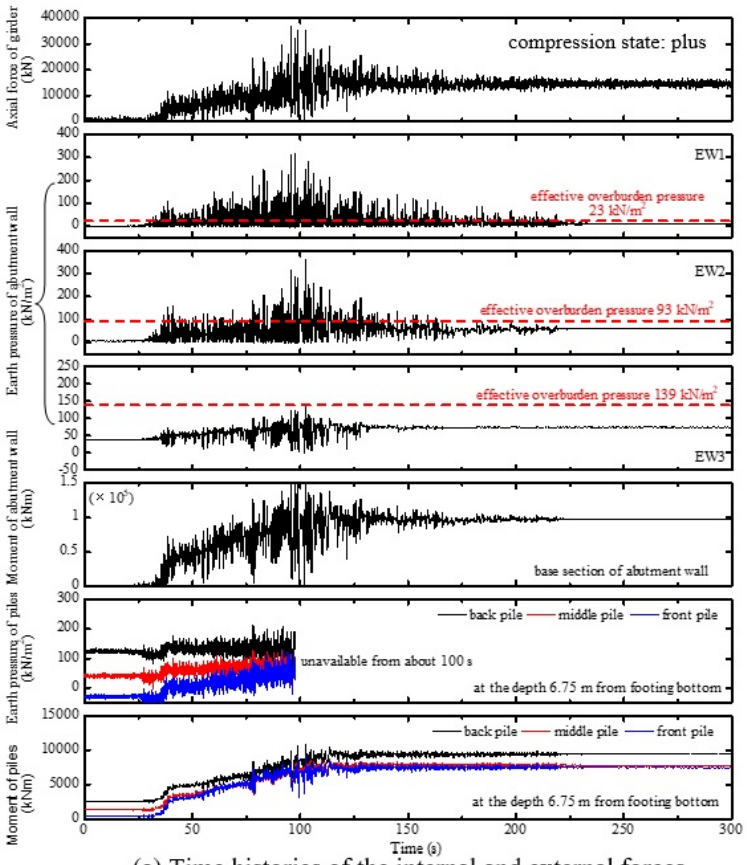

(a) Time histories of the internal and external forces

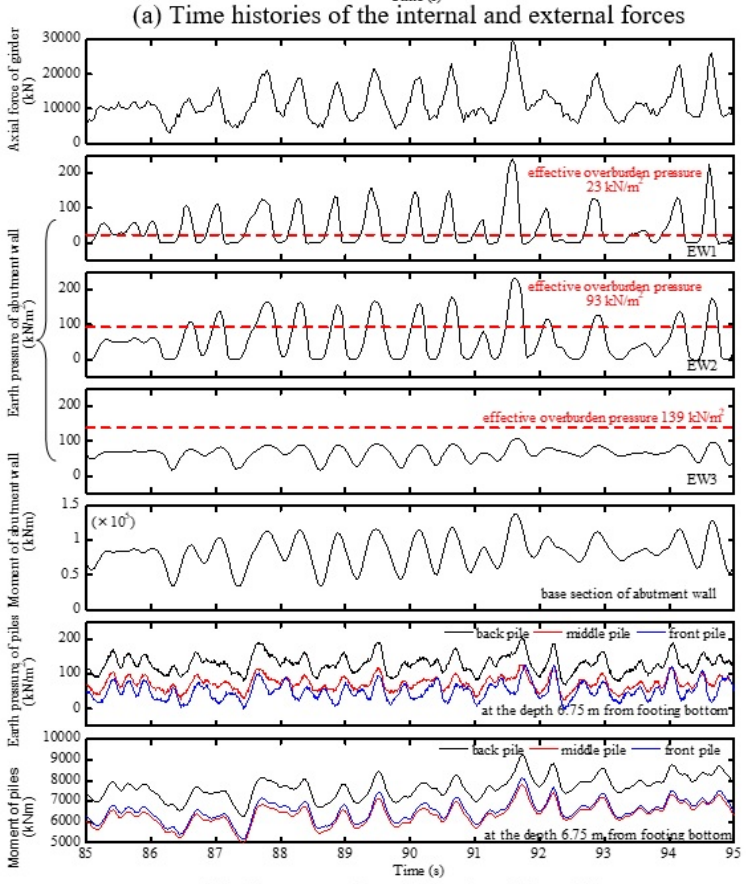

(b) Close-up view from time 85 to 95 s

Figure 13 Comparison between the time histories of the internal and external forces

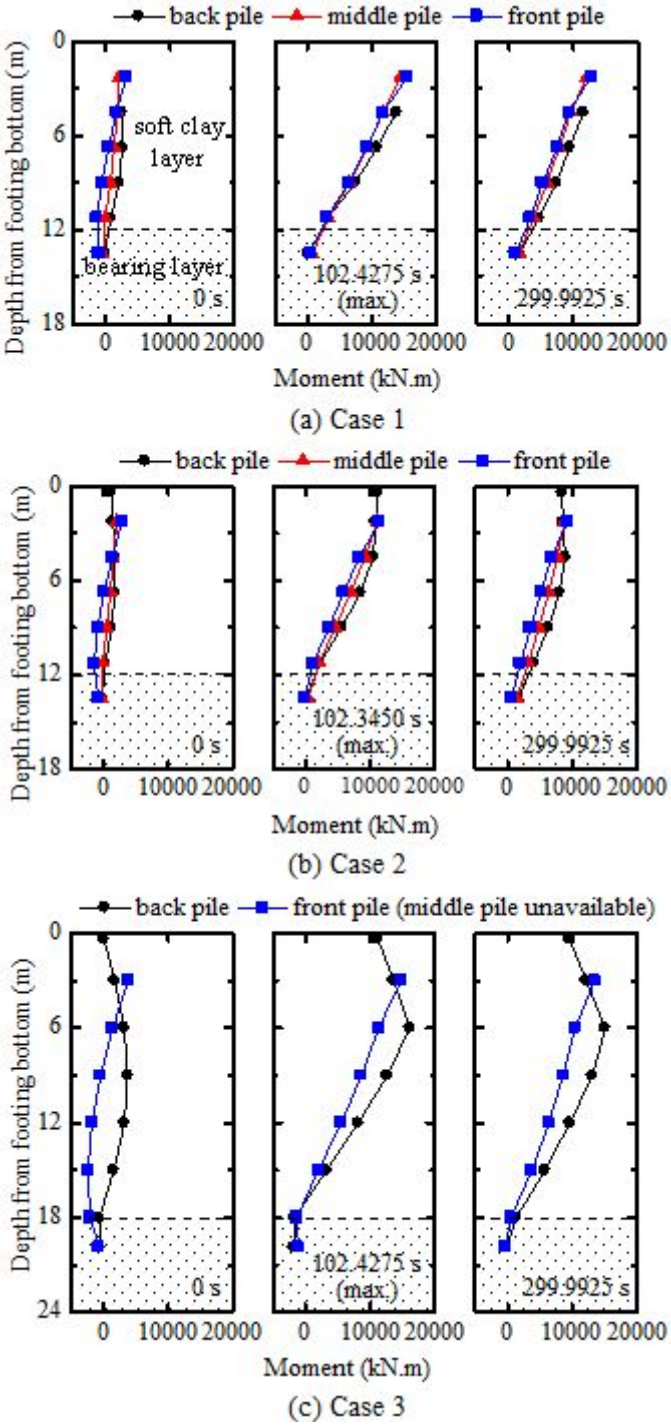

Figure 14 Pile bending moment distributions

5. CONCLUSIONS

To investigate the bridge seismic behavior subjected to the earthquake-induced lateral movement of the soft clay layer, the pile-supported bridge abutments located on the soft clay deposits, with different materials and thicknesses, at the movable bearing side are modeled, and dynamic centrifuge experiments are conducted in a 75 g field. The following major conclusions are obtained.

1. Under the effect of the earthquake-induced lateral movement of the soft clay layer, both the settlement at the back-side ground surface and the lateral displacement at the front-side ground surface near the bridge abutment wall are clearly larger than those at other locations. The results also show that the shear strength and the thickness of the soft clay layer can considerably affect the ground seismic displacement behavior.

2. The bridge abutment wall is restrained at the top position due to the collision with the girder; however, due to the lateral movement of the soft clay layer, the footing largely moves forward, resulting in a large backward inclination of the bridge abutment. Furthermore, it is confirmed that the shear strength and the thickness of the soft clay layer can considerably affect the rotation angle of the bridge abutment.
3. It is found that due to the lateral movement of the soft clay layer, the pile bending moment considerably increases during base shaking and generally persists, even at the end of base shaking. It is also confirmed that the bending moment acting on the back-row pile is larger than those acting on the middle- and front-row piles.
4. In the case that the soft clay layer has high shear strength, the ground lateral movement may cause a high external earth pressure on the piles, although the ground displacement is relatively small. Furthermore, due to the non-uniform ground lateral movement with depth, especially in the thick soft clay layer, the high pile earth pressure may occur locally, rather than along the whole pile length.

In the near future, numerical simulation analysis will be conducted for dynamic centrifuge experiments. The evaluation method for the seismic performance of the existing bridges, which are potentially subjected to the lateral movement of the soft clay layer during an earthquake, will be developed based on the experimental and numerical results.

Acknowledgments

This study is supported by the “DEVELOPMENT OF SEISMIC TECHNOLOGY FOR STRENGTHENING EARTHQUAKE RESILIENCE OF INFRASTRUCTURE FACILITIES” project, conducted at the Public Works Research Institute of Japan from 2016 to 2021. The support is gratefully acknowledged.

Author’s Contributions: Conceptualization, S Tanimoto and Y Yang; Methodology, S Tanimoto and Y Yang; Investigation, Y Yang and S Tanimoto; Writing - original draft, Y Yang; Writing - review and editing, Y Yang, S Tanimoto, and T Kiriyama; Funding acquisition, T Kiriyama; Resources, T Kiriyama; Supervision, T Kiriyama.

Editor: Marcílio Alves.

References

Banerjee, S., Goh, S.H., Lee, F.H. (2014). Earthquake-induced bending moment in fixed-head piles in soft clay. Géotechnique 64:431–446.

Boominathan, A., Ayothiraman, R. (2006). Dynamic response of laterally loaded piles in clay. Proceedings of the Institution of Civil Engineers-Geotechnical Engineering 159:233–241.

Boulanger, R.W., Curras, C.J., Kutter, B.L., Wilson, D.W., Abghari, A. (1999). Seismic soil-pile-structure interaction experiments and analyses. Journal of Geotechnical and Geoenvironmental Engineering 125:750–759.

Brandenberg, S.J., Boulanger, R.W., Kutter, B.L., Chang, D. (2005). Behavior of pile foundations in laterally spreading ground during centrifuge tests. Journal of Geotechnical and Geoenvironmental Engineering 131:1378–1391.

Brown, D.A., O Neill, M., Hoit, M., McVay, M., El Naggar, M., Chakraborty, S. (2001). Static and Dynamic Lateral Loading of Pile Groups, TRB (Washington, DC, USA).

Chandrasekaran, S., Boominathan, A., Dodagoudar, G. (2010). Experimental investigations on the behaviour of pile groups in clay under lateral cyclic loading. Geotechnical and Geological Engineering 28:603–617.

Chang, D. (2007). Inertial and lateral spreading demands on soil-pile-structure systems in liquefied and laterally spreading ground during earthquakes, Ph.D. Dissertation, University of California, Davis.

El-Sekelly, W., Abdoun, T., Dobry, R. (2016). PRESHAKE: a database for centrifuge modeling of the effect of seismic preshaking history on the liquefaction resistance of sands. Earthquake Spectra 32:1925–1940.

Fleming, B.J., Sritharan, S., Miller, G.A., Muraleetharan, K.K. (2016). Full-scale seismic testing of piles in improved and unimproved soft clay. Earthquake Spectra 32:239–265.

Garala, T.K., Madabhushi, G.S. (2019). Seismic behaviour of soft clay and its influence on the response of friction pile foundations. Bulletin of Earthquake Engineering 17:1919–1939.

Japan Road Association. (2017). Design specifications of highway bridges. JRA (in Japanese) (Tokyo, Japan).

Madabhushi, G. (2014). Centrifuge Modelling for Civil Engineers, CRC Press (Boca Raton, Florida, United States).

Mayoral, J.M., Alberto, Y., Mendoza, M.J., Romo, M.P. (2009). Seismic response of an urban bridge-support system in soft clay. Soil Dynamics and Earthquake Engineering 29:925–938.

Mayoral, J.M., Pestana, J.M., Seed, R.B. (2005). Determination of multidirectional p-y curves for soft clays. Geotechnical Testing Journal 28:253–263.

Meymand, P.J. (1998). Shaking table scale model tests of nonlinear soil-pile-superstructure interaction in soft clay, Ph.D. Dissertation, University of California, Berkeley.

Port and Airport Research Institute. (2003). Lateral Resistance of Soft Landing Moundless Structure with Piles. Technical Note, No. 1039, PARI (in Japanese) (Kanagawa, Japan).

Public Works Research Institute. (2014). Reconnaissance Report on Damage to Road Bridges by the 2011 Great East Japan Earthquake. Technical Note, No. 4295, PWRI (in Japanese) (Tsukuba, Japan).

Public Works Research Institute. (2018). Damage Mechanism Investigation for Bridges Failed in the 2011 Tohoku-Oki Earthquake of Japan Using FEM Analysis. Technical Note, No. 4367, PWRI (in Japanese) (Tsukuba, Japan).

Qiu, Z., Ebeido, A., Almutairi, A., Lu, J., Elgamal, A., Shing, P.B., Martin, G. (2020). Aspects of bridge-ground seismic response and liquefaction-induced deformations. Earthquake Engineering & Structural Dynamics:1–19. doi: 10.1002/eqe.3244.

Rollins, K.M. and Brown, D.A. (2011). Design Guidelines for Increasing the Lateral Resistance of Highway-Bridge Pile Foundations by improving Weak Soils, Transportation Research Board (Washington, D.C., United States).

Schofield, A.N. (1980). Cambridge geotechnical centrifuge operations. Geotechnique 30:227–268.

Shirato, M., Fukui, J., Koseki, J. (2006). Current status of ductility design of abutment foundations against large earthquakes. Soils and foundations 46(3): 377-396.

Su, L., Tang, L., Ling, X., Liu, C., Zhang, X. (2016). Pile response to liquefaction-induced lateral spreading: a shake-table investigation. Soil Dynamics and Earthquake Engineering 82:196–204.

Wilson, D.W. (1998). Soil-pile-superstructure interaction in liquefying sand and soft clay, Doctoral Dissertation, University of California, Davis.

Wilson, D.W., Boulanger, R.W., Kutter, B.L. (1997). Soil-Pile-Superstructure Interaction at Soft or Liquefiable Soil Sites - Centrifuge Data Report for CSP4, Report No. UCD/CGMDR-97/05, Center for Geotechnical Modeling, Department of Civil and Environmental Engineering, University of California (Davis).

Wilson, D.W., Boulanger, R.W., Kutter, B.L. (2000). Observed seismic lateral resistance of liquefying sand. Journal of Geotechnical and Geoenvironmental Engineering 126:898–906.

Yang, J., Yang, M., Chen, H. (2019). Influence of pile spacing on seismic response of piled raft in soft clay: centrifuge modeling. Earthquake Engineering and Engineering Vibration 18:719–733.

Zhang, L., Goh, S., Yi, J. (2017). A centrifuge study of the seismic response of pile–raft systems embedded in soft clay. Géotechnique 67:479–490.

Zhang, X., Tang, L., Li, X., Ling, X., Chan, A. (2020). Effect of the combined action of lateral load and axial load on the pile instability in liquefiable soils. Engineering Structures 205:110074.